Visible cathodoluminescence of Er ions in β-Ga_2O_3 nanowires and microwires

2008 Nanotechnology 19 035713

(http://iopscience.iop.org/0957-4484/19/3/035713)

Nanotechnology **19** (2008) 035713 (4pp) doi:10.1088/0957-4484/19/03/035713

Visible cathodoluminescence of Er ions in β-Ga_2O_3 nanowires and microwires

E Nogales, B Méndez and J Piqueras

Departamento de Física de Materiales, Facultad de Ciencias Físicas, Universidad Complutense de Madrid, 28040 Madrid, Spain

E-mail: bianchi@fis.ucm.es (B Méndez)

Received 12 September 2007, in final form 19 November 2007
Published 14 December 2007
Online at stacks.iop.org/Nano/19/035713

Abstract

Erbium doped β-Ga_2O_3 nanowires and microwires have been obtained by a vapour–solid process from an initial mixture of Ga_2O_3 and Er_2O_3 powders. X-ray diffraction (XRD) analysis reveals the presence of erbium gallium garnet as well as β-Ga_2O_3 phases in the microwires. Scanning electron microscopy (SEM) images show that the larger microwires have a nearly rectangular cross-section. Transmission electron microscopy (TEM) and high-resolution TEM (HRTEM) analysis show good crystal quality of the β-Ga_2O_3 nanowires. The nanostructures have been studied by means of the cathodoluminescence technique in the scanning electron microscope. Er intraionic blue, green and red emission lines are observed in luminescence spectra even at room temperature, which confirms the optical activity of the rare earth ions in the grown structures. Mapping of the main 555 nm emission intensity shows a non-homogeneous distribution of Er ions in the microstructures.

1. Introduction

Functional nanowires are considered as a well defined class of building blocks which can be used to form more complex structures with a number of potential applications in nanotechnology [1, 2]. Among different semiconductor oxides, monoclinic gallium oxide (β-Ga_2O_3) is a very promising material for optoelectronic applications due to its wide band gap (around 4.9 eV) which allows one to tune the emission wavelength from the ultraviolet to the infrared regions of the spectrum [3, 4]. Several works devoted to the synthesis [5–8] and the luminescence from red to UV [9–11] of β-Ga_2O_3 nanowires have been published in the past years. The research field is still in its infancy and problems such as doping or the origin of certain luminescence bands are still under investigation. Rare earth (RE) ions embedded into wide band gap semiconductor hosts have attracted interest due to their narrow emission lines in the visible and infrared range, which are usually independent of the host matrix [12–15]. One of the problems is the thermal quenching of the RE emission at room temperature, which seems to be less noticeable for wide band gap hosts [16]. Therefore, β-Ga_2O_3 is a suitable choice as matrix material for RE elements, and some works related to optical characterization of thin films of Ga_2O_3 doped with Eu and Dy have been reported [17–19]. However, the study of the emissions from RE ions in Ga_2O_3 nanowires has not yet been performed, to our knowledge. In our group, we have recently successfully applied a vapour process method to obtain elongated nanostructures of different semiconductor oxides, such as ZnO, GeO_2, SnO_2, Ga_2O_3 and others [9, 20–22]. The aim of the present work is to apply this method to grow erbium doped Ga_2O_3 nanowires, and to study their luminescence behaviour, which is expected to be of interest in optoelectronic nanodevices.

In this work, we present a structural and luminescence study of β-Ga_2O_3 microwires and nanowires containing erbium, which are obtained by sintering pellets made with a Ga_2O_3 and Er_2O_3 mixed powder. The growth process leads to the formation of erbium gallium garnet (EGG) as well as Er doped β-Ga_2O_3. The light emission properties have been studied by means of the cathodoluminescence (CL) in the visible range, which shows the characteristic emission lines arising from Er^{3+} intra 4f shell transitions in the obtained nanostructures.

2. Experimental details

Samples were prepared from mixtures of pure Ga_2O_3 and Er_2O_3 powders, which were mechanically milled for 30 h. Two mixtures, with 5% and 20% of Er_2O_3, were used as precursor

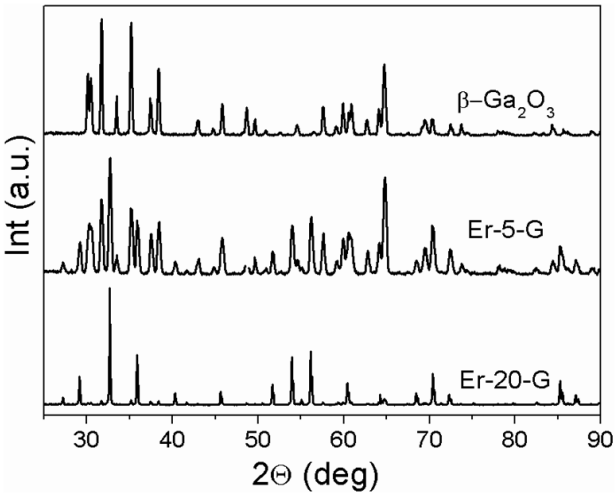

Figure 1. XRD patterns of samples Er-5-G, Er-20-G and β-Ga_2O_3. Peaks corresponding to monoclinic gallium oxide (β-Ga_2O_3) and erbium gallium garnet ($Er_3Ga_5O_{12}$) have been identified in the former two samples.

materials. The samples obtained from these mixtures were labelled as Er-5-G and Er-20-G, respectively. The compacted mixture was annealed under argon flow either with one or with two temperature step treatments. The single step was carried out at 1500 °C for 15 h. In the two-step treatment an annealing at 1500 °C for 5 h was followed by a second one at 1350 °C for 5 h. Both processes led to the formation of nanostructures on the surface of the pellet without the use of a catalyst, as detailed elsewhere [9, 20–22]. The resulting samples were characterized by means of x-ray diffraction (XRD) to assess the crystalline structure. Transmission electron microscopy (TEM), high-resolution TEM (HRTEM) and selected area electron diffraction (SAED) analyses were performed with JEOL JEM 2000FX and JEM 3000F microscopes. In order to analyse individual wires, sonication was carried out for TEM observation. The morphology and CL investigations of the obtained structures were carried out in a SEM Leica Steroscan 440. CL measurements were performed in the visible range between 88 and 300 K using accelerating voltages of 15 or 20 kV. CL images and spectra were acquired with Hamamatsu photon counting and CCD systems, respectively.

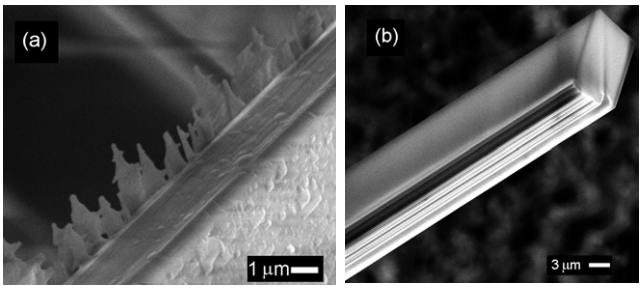

Figure 3. SEM micrographs of sample Er-20-G obtained by (a) two-step and (b) single-step treatments.

3. Results and discussion

The XRD spectra from the final nanostructures reveal the presence of erbium gallium garnet (EGG), $Er_3Ga_5O_{12}$, as well as monoclinic gallium oxide, β-Ga_2O_3, phases in Er-5-G and Er-20-G samples (figure 1). No peaks related with Er_2O_3 were observed. SEM images show the formation of nanostructures, mainly in the form of rods, wires and planar sheets with dimensions in the range of micrometres and nanometres. Figure 2(a) shows the structures obtained in the surface of sample Er-5-G, after a two-step thermal treatment. The secondary electron image shows tetragonal rods with aligned needles emerging from some faces. Figure 2(b) shows a detail of the surface with nanostructures. They present widths ranging from a few tens to a few hundreds of nanometres and lengths of a few microns. For comparison, the same two-step temperature treatment was applied to pure Ga_2O_3 powders and parallel nanowires and comb-like structures were developed on the surface, as is shown in figure 2(c). In the case of the highest Er_2O_3 content, sample Er-20-G, rectangular plates and rods with similar structures on the surface were formed, as can be seen in figure 3(a). Nanowires, plates and microrods were also obtained in samples with a single-step temperature treatment, but the faces of the microstructures are wire-free (see figure 3(b)). From the above images, the two-step thermal treatment seems to favour the growth of small needles from the lateral faces of the microrods, which is not observed in a one-step annealing. This may apply either to undoped Ga_2O_3 or to Er doped Ga_2O_3. However, in the latter case, the growth process develops rods with nearly rectangular cross-sections, as figures 2(a) and 3(b) show. The size of these rods varies from

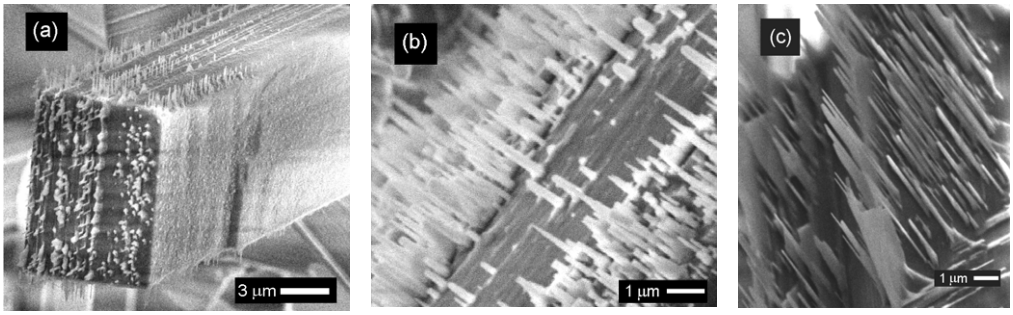

Figure 2. SEM micrographs of (a) nanostructures formed in sample Er-5-G, (b) detail of the surface of a rod, and (c) nanowires in an undoped Ga_2O_3 sample. Both samples have been obtained following a two-step thermal treatment.

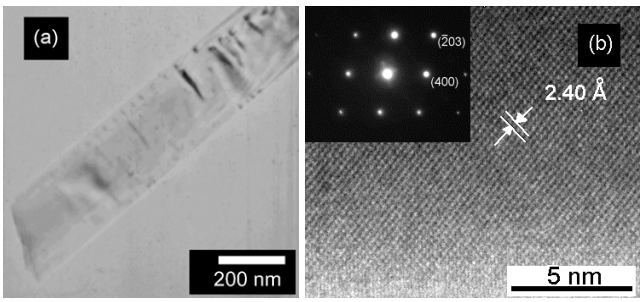

Figure 4. (a) TEM image of a nanowire around 250 nm wide from sample Er-5-G and (b) HRTEM image of the wire showing the good crystal quality and the distance which corresponds to the (401) β-Ga_2O_3 plane. The inset shows the SAED pattern, which corresponds to the [010] β-Ga_2O_3 zone axis.

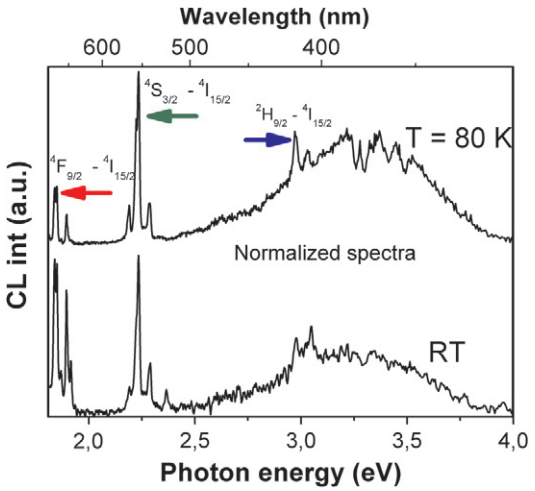

Figure 5. CL spectra from sample Er-20-G at 88 K and at room temperature (RT) from the nanostructures. They are also representative of the spectra obtained in sample Er-5-G. Er intraionic emission lines are indicated by the arrows.

10–20 μm to less than 1 μm. In the case of undoped Ga_2O_3 annealed under argon flow in a single-temperature treatment, the structures tend to be different, such as elongated wires and comb-like structures [9]. The presence of nanowires grown on the faces of microrods of samples grown with two temperature steps and not with a single step indicates that they are formed during the 1350 °C step, lower than the 1500 °C of the first one. It is well known [23] that the morphology of the wires, including the length/width ratio, depends on the different planes' surface energies, which depend on the growth temperature.

Figure 4(a) shows a TEM image of a nanowire about 250 nm wide from sample Er-5-G. The HRTEM image, figure 4(b), shows the high crystal quality of the wire shown in 4(a). The indicated interplanar distance corresponds to the (401) β-Ga_2O_3 crystal planes. The SAED pattern in the inset, along the [010] β-Ga_2O_3 zone axis, shows that the wire is monocrystalline. No presence of particles with EGG structure was observed in the TEM images of the nanowires with these dimensions.

In order to study the influence of Er ions in the optical properties of the obtained nanostructures, CL measurements were performed. These include luminescence mapping and CL spectra from the nanostructures in the visible range. The well known sharp emission lines arising from Er^{3+} intra 4f shell transitions are recorded from the microstructures and nanostructures even at room temperature, along with emission bands related to the β-Ga_2O_3 matrix. Figure 5 shows the CL spectra from sample Er-20-G at 88 K and at room temperature. It has been found that the Er^{3+} emission intensity from nanowires is almost independent of the Er_2O_3 content in the starting powder (5% or 20%). At low temperature, the CL spectrum shows the typical broad UV–blue band previously found in β-Ga_2O_3 single crystals by photoluminescence measurements and attributed to donor–acceptor-pair (DAP) transitions involving oxygen vacancies [4, 8, 24]. Besides this emission, three sets of lines, labelled in the figure, are clearly resolved in the CL spectrum at around 420, 555 and 660 nm, which correspond to some of the Er^{3+} 4f intraionic transitions [12]. For example, in Er doped GaN, Steckl *et al* [13] have reported strong green (537–558 nm) lines associated with erbium intraionic transitions. The broad blue band is slightly quenched as the temperature increases and at room temperature the green and red peaks from Er^{3+} ions dominate the CL spectrum. By considering the relative intensities of Er^{3+} emissions in figure 5, it can be seen that the ratio between the CL intensity of red and green lines changes from low to room temperature. The red lines have similar intensity at room temperature as the green ones. This behaviour has been observed in erbium on silicon [14], and it was related to the presence of erbium ions surrounded by oxygen atoms, which is also the case in the β-Ga_2O_3 and EGG lattices.

We have also used CL monochromatic images to study the Er distribution in the structures. Figure 6(a) shows an SEM micrograph of a region of the sample Er-20-G and figure 6(b) shows the green cathodoluminescence mapping of the same area at liquid nitrogen temperature. The observed contrast in the SEM image reveals topographic features in the plates. It can be observed from figure 6(b) that Er^{3+} green emission is enhanced in parallel stripes inside the rectangular plates, which indicates an inhomogeneous Er ion concentration in the gallium oxide matrix. The monochromatic CL image from sample Er-5-G reveals the presence of some clusters with a stronger Er emission than the rest of the wire (figure 6(c)). From the fact that the Er concentration is much higher in EGG than in doped Ga_2O_3, we suggest that these clusters are formed by EGG. These results show that the incorporation of Er is not homogeneous inside the planar structures, as the erbium oxide concentration increases. The strong green luminescence obtained from the nanostructures demonstrates that erbium ions have been effectively incorporated into the nanostructures and are optically active centres. The thermal treatment performed to grow the nanostructures serves also for optical activation for Er ions. The fabrication method used to grow the nanostructures enables us to get RE doped nanostructures without the need of a further activation process. This method could be extended to other RE elements such as Eu or Yb in a gallium oxide matrix in order to achieve

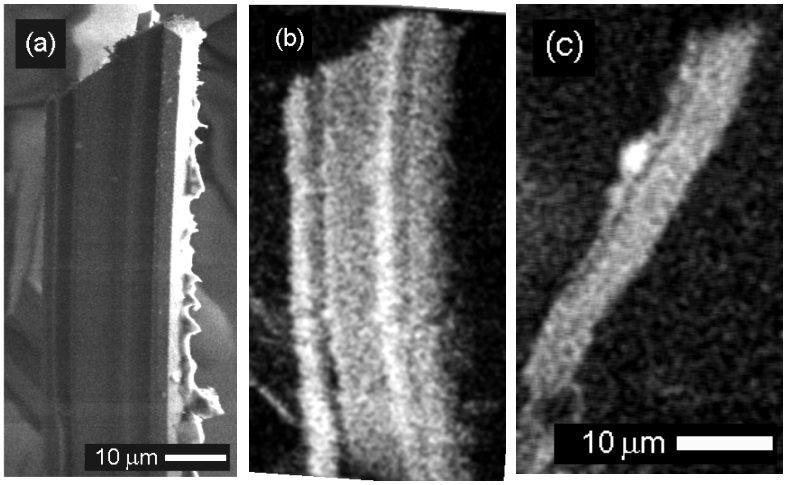

Figure 6. (a) SEM image from sample Er-20-G at 88 K. (b) Monochromatic CL image at 555 nm of the same area. (c) Monochromatic CL image at 555 nm from sample Er-5-G.

intraionic luminescence at selective wavelengths from the specific RE ions within Ga_2O_3 nanowires.

4. Conclusions

Erbium doped β-Ga_2O_3 nanostructures and microstructures have been obtained through thermal treatment of mixed Ga_2O_3 and Er_2O_3 powders. Nearly rectangular rods and plates with or without aligned needles grown on some of their faces were obtained depending on the two-step or single-step temperature treatments of the samples, respectively. TEM, HRTEM and SAED studies show nanowires with very good crystal quality with a homogeneous β-Ga_2O_3 structure obtained by a catalyst-free method. In all cases, the presence of rather intense Er emission lines, even at room temperature, is observed in the CL spectra. The results show that vapour–solid process is an efficient method to produce Er luminescent nanostructures based on gallium oxide.

Acknowledgment

This work has been supported by MEC (Project MAT 2003-00455).

References

[1] Lieber C M and Wang Z L 2007 *MRS Bull.* **32** 99
[2] Lu J G, Chang P and Fan Z 2006 *Mater. Sci. Eng.* R **52** 49
[3] Tippins H H 1965 *Phys. Rev.* **140** A316
[4] Binet L and Gourier D 1998 *J. Phys. Chem. Solids* **59** 1241
[5] Zhang H Z, Kong Y C, Wang Y Z, Du X, Bai Z G, Wang J J, Yu D P, Ding Y, Hang Q L and Feng S Q 1999 *Solid State Commun.* **109** 677
[6] Song Y P, Zhang H Z, Lin C, Zhu Y W, Li G H, Yang F H and Yu D P 2004 *Phys. Rev.* B **69** 075304
[7] Choi Y C, Kim W S, Park Y S, Lee S M, Bae D J, Lee Y H, Park G-S, Choi W B, Lee N S and Kim J M 2000 *Adv. Mater.* **12** 746
[8] Kim H W 2007 *Appl. Phys.* A **86** 315
[9] Nogales E, Méndez B and Piqueras J 2005 *Appl. Phys. Lett.* **86** 113112
[10] Nogales E, García J A, Méndez B and Piqueras J 2007 *J. Appl. Phys.* **101** 033517
[11] Zhou X T, Heigl F, Ko J Y P, Murphy M W, Zhou J G, Regier T, Blyth R I R and Sham T K 2007 *Phys. Rev.* B **75** 125303
[12] Gruber J B, Henderson J R, Muramoto M, Rajnak K and Conway J G 1966 *J. Chem. Phys.* **45** 477
[13] Steckl A J and Birkhan R 1998 *Appl. Phys. Lett.* **73** 1700
[14] Nogales E, Méndez B, Piqueras J, Plugaru R, Coraci A and García J A 2002 *J. Phys. D: Appl. Phys.* **35** 295
[15] Wang K, Martin R W, Nogales E, Edwards P R, O'Donnel K P, Lorenz K, Alves E and Watson I M 2006 *Appl. Phys. Lett.* **89** 131912
[16] Favennec P N, Haridon H L, Salvi M, Muotonnet D and Le Guillo Y 1989 *Electron. Lett.* **25** 718
[17] Gollakota P, Dhawan A, Wellenius P, Lunardi L M, Muth J F, Saripalli Y N, Peng H Y and Everitt H O 2006 *Appl. Phys. Lett.* **88** 221906
[18] Pang M L, Shen W Y and Lin J 2005 *J. Appl. Phys.* **97** 033511
[19] Hao J and Cocivera M 2002 *J. Phys. D: Appl. Phys.* **35** 433
[20] Grym J, Fernández P and Piqueras J 2005 *Nanotechnology* **16** 931
[21] Hidalgo P, Méndez B and Piqueras J 2005 *Nanotechnology* **16** 2521
[22] Maestre D, Cremades A and Piqueras J 2005 *J. Appl. Phys.* **97** 044316
[23] Cui Y, Duan X, Huang Y and Lieber C M 2003 *Nanowires and Nanobelts, Materials, Properties* vol I, ed Z L Wang (Berlin: Springer) pp 3–65
[24] Villora E G, Atou T, Sekiguchi T, Sugawara T, Kikuchi M and Fukuda T 2001 *Solid State Commun.* **120** 455